

Effects of Neutron Irradiation on Advanced CrNiMoV Reactor Pressure Vessel Steel

R. Havel, M. Vacek, P. Novosad

Nuclear Research Institute, Rez (near Prague), Czechoslovakia

1. INTRODUCTION

The Cr-Ni-Mo-V steel 15Ch2NMFA is used for manufacturing of pressure vessels of four loop pressurized water reactors VVER1000 in the USSR since 1980. Within the framework of cooperation in production of nuclear power plant components these pressure vessels are produced also in the SKODA Corporation, Czechoslovakia. Extensive qualification programme was designed to prove appropriate properties of czechoslovak made reactor pressure vessel steel 15Ch2NMFA, Grade AA, including its resistance to radiation damage, /Brumovský, 1987/.

The pressure vessel is manufactured from forged rings joined by submerged arc welds. For the first three VVER1000 pressure vessels produced the evaluation of irradiation stability was prescribed for beltline region /three rings for each vessel/. The calculated end of life fluence on the pressure vessel wall of VVER1000 type reactor is $6.5 \times 10^{23} \text{ n m}^{-2}$ for $E > 0.5 \text{ MeV}$ what corresponds to $3.3 \times 10^{23} \text{ n m}^{-2}$, $E > 1 \text{ MeV}$ at irradiation temperature 290-10 deg C. Accelerated irradiation of beltline region material was carried out up to fluences equal or even exceeding the above mentioned end of life fluence.

Irradiation hardening in terms of yield stress increase, transition temperature shifts in terms of Charpy impact energy levels and fracture toughness together with upper shelf drop due to neutron irradiation were evaluated after irradiation in experimental reactor up to neutron fluences of $4.6 \times 10^{23} \text{ n m}^{-2}$, $E > 1 \text{ MeV}$.

2. MATERIAL

192 mm thick forged rings of outer diameter 4535 mm were produced commercially from 170 tons ingots using selected batch of PVK cast iron of high purity. After austenitising at 960 deg C/air, forgings were water quenched from 920 deg C and tempered at 650 deg C/air. Chemical composition of the 15Ch2NMFA Grade AA steel for each of three heats A, B, C examined is given in Table 1.

Charpy-V and pre-cracked Charpy specimens were taken from the heads of the rings in 1/3 of thickness with the C-L orientation, longitudinal axis of tensile specimens was perpendicular to crack propagation plane. The experimental material have received simulated post-weld heat treatment /620 deg C/20h followed by 650 deg C/10h/furnace/. The microstructure of investigated material is a mixture

of tempered bainite and martensite, Fig.1., as follows from the heat treatment conditions. Specimens for fracture toughness testing were fatigue pre-cracked to an a/W ratio of 0.55 and subsequently sidegrooved with Charpy V-notch cutter to the depth of 0.1B.

3. IRRADIATION CONDITIONS

Irradiation was carried out in LWR pool type experimental reactor VWR-S using electrically heated irradiation rig Chouca-M located inside the core. Neutron flux during irradiation was $1.3 \times 10^{17} \text{ n m}^{-2} \text{ s}^{-1}$, $E > 1 \text{ MeV}$.

Neutron fluence was evaluated using reaction $\text{Cu}^{63} \rightarrow \text{Co}^{60}$ with respect to measured neutron spectrum; neutron fluences were evaluated with uncertainty less than 20 %, /Ošmera, 1982/.

Temperature during irradiation was monitored and controlled using thermocouples, it was held at 285-12 deg C, /Pina, 1988/.

4. EXPERIMENTAL PROCEDURES

Tensile properties were measured on specimens of 4 mm diameter, 20 mm length at ambient temperature using $4.2 \times 10^{-3} \text{ s}^{-1}$ deformation rate.

Charpy impact energy levels were measured using standard testing methods and equipment with working capacity 294 J and tup velocity 5.6 m/s within the temperature range -160 to +200 deg C. The test temperature was measured and controlled with accuracy better than ± 2 deg C.

Fracture toughness tests were performed within the temperature range -190 to +200 deg C according to the methodology of the corresponding INTERATOMENERGO standard /NID IAE, 1986/ with slight deviations due to the use of subsized pre-cracked Charpy specimens and specific conditions for the work with irradiated materials, as described elsewhere /Havel, 1989/. Within the whole temperature range sidegrooved specimens and unloading compliance method were used ie. there were some unnecessary partial unloadings performed in the brittle and transition region. Load point displacement was measured remotely using LVDT gauges mounted across the loading jig, correction function was used to account for extraneous displacement, resulting from elastic and plastic deformation of loading jig and specimen /Neale, 1985/. This method yields comparable or even better results than the use of clip gauge due to the higher linearity of LVDT gauges and is favourable especially for remote handling and non-ambient temperatures testing. Initiation toughness values were evaluated according to following formulas:

$$K_{IC} = \frac{P.F/a/W/.L}{/B.B_n/^{1/2} .W^{3/2}} \quad \dots \text{ brittle region}$$

$$K_{JC}^2 = \frac{E}{1 - \nu^2} J_C \quad \dots \text{ transition region}$$

$$K_{O.2}^2 = \frac{E}{1 - \nu^2} J_{O.2} \quad \dots \text{ ductile region}$$

where $J_{0.2}$ is the value corresponding to 0.2 mm of crack growth on the $J - \Delta a$ curve and J_C the value of J , corresponding to the initiation of unstable fracture, preceded by plastic deformation without or with negligible crack growth / a 0.2 mm/. Both these J values were evaluated using standard formulas with the area under load-displacement record divided into elastic and plastic part /NTD IAE, 1986/. Power law fit was used for the $J - \Delta a$ curve. The $J_{0.2}$ value is an approximation to the true initiation value, as proposed in the CEGB procedure /Neale et.al., 1984/.

5. RESULTS

5.1. Tensile properties

Tensile properties, measured at ambient temperature, are given for both unirradiated and irradiated specimens in Table 2. where parameter B_F , defined:

$$\Delta R_{p0.2} = B_F / F \times 10^{-22} \text{ n m}^{-2} / 1/3$$

is also given. B_F is characterizing the irradiation hardening resistance at given temperature. The values of tensile properties are mean values, obtained from several measurements.

5.2. Charpy impact energy levels

Measured Charpy impact energy levels are given for the heat B in Figure 2. with the impact energy/temperature relationship fitted to the data in the form /Oldfield, 1975/:

$$KV/T/ = 1 + M \tanh / \frac{T - T_0}{N} /$$

Transition temperatures and upper shelf energy values, obtained using this relationship, are summarized for each heat examined in Table 3., where the values of parameter A_F , defined as:

$$\Delta TT = A_F / F \times 10^{-22} \text{ n m}^{-2} / 1/3$$

are also given.

5.3. Fracture properties

Due to the small specimen size /10x10x55/ significant size effects and scatter of the data were expected. The results of unirradiated sidegrooved pre-cracked Charpy specimens are compared with the data of Janda and Mentl, 1988, obtained using 75 mm thick plain sided compact tension specimen, Fig. 3. Toughness/temperature relationship was used in the form:

$$K_C /T/ = K_0 + P \exp QT \quad \dots \text{ transition region}$$

$$K_C /T/ = R + ST \quad \dots \text{ upper shelf}$$

Results of initiation toughness tests for both unirradiated and irradiated specimens are given in Figures 4.-6. Transition temperatures, upper shelf initiation toughness levels and their changes due to irradiation for each heat examined are summarized in Table 4., where the values of parameter ΔK_F , defined as:

$$\Delta TT_{100} = A_F^K / F \times 10^{-22} \text{ n m}^{-2} / 1/3$$

are also given. The transition temperature shifts were evaluated at the level $100 \text{ MPa m}^{1/2}$, the upper shelf initiation toughness drop at temperature of the onset of upper shelf of irradiated specimen.

The use of $J_{0.2}$ as an approximation of initiation value of J was confirmed for this type of steel by stretch zone width measurement using SEM fractography. Measured values of stretch zone width were ranging from 0.16 to 0.25 mm for specimens tested on the upper shelf temperatures.

6. DISCUSSION

Observed values of irradiation hardening were found to be within expected limits for both fluences used. Measured elongation and contraction were above 17 % and 74 % respectively, the ratio $R_{p0.2}/R_m$ increased from 0.85 to 0.91 due to irradiation. This indicates that there is sufficient plasticity available even after irradiation with higher fluences. The value of parameter B_F was found to increase with neutron fluence.

The transition temperature shift, evaluated from Charpy test is the most common measure of irradiation embrittlement. There were no significant differences observed between examined steels. The transition temperatures shifts for heats A, B, C were found to decrease in quoted order, conversely reversed relation was found for the upper shelf energy levels. This could be accounted to the insufficient number of data on the upper shelf. Irradiation embrittlement in terms of transition temperature shift is within acceptable limits even for fluences exceeding the end of life fluence. The same is valid for the upper shelf, where the lowest value of upper shelf energy measured was 223 Jcm^{-2} for heat C.

The tendency of A_F to increase with the increasing fluence, which was also found for B_F in the case of tensile properties suggests, that proposed relationship, i.e. value of exponent $n = 1/3$, is not completely valid. Analysis of the data revealed, that more realistic description of irradiation induced changes could be made using equations:

$$\Delta R_{p0.2} = 55 / F \times 10^{-22} / 0.82$$

and

$$\Delta TT_{41J} = 25 / F \times 10^{-22} / 0.76$$

Substantially higher values of exponent n compared with recommended $1/3$ indicates that much lower level of saturation effects of radiation damage than expected was observed for this type of steel and employed irradiation conditions. Negligible differences in the measured values of corresponding constants could result from error level in irradiation parameters evaluation.

Significant effect of specimen size was observed in the transition region of the initiation toughness/temperature relationship, Fig. 3. Various models,

accounting for specimen size /thickness/, which were published recently were not applied because of considerable scatter and insufficient data available. As there were no systematic effects of specimen size reported on the upper shelf /Ingham et.al., 1983, Bolton, 1987/, the evaluation of size effects on the temperature of the onset upper shelf could be of main importance for the design or assessment purposes. It is recognized, that both stress/strain fields ahead of the crack tip /specimen geometry and size/ and fracture process initiation sites distribution /material/ have the most significant role. However, it should be noted that the pre-cracked Charpy results are used as a measure of irradiation induced fracture properties changes only and these changes are evaluated from values, obtained using specimens of the same type and size.

Figures 4. to 7. are summary plots of initiation toughness for heats examined. The initiation toughness/temperature curves were almost indistinguishable for all three heats in unirradiated state. Measured transition temperature shifts are to some point consistent with the Charpy impact tests results. Considerable scatter, observed in the transition region suggests, that more appropriate would be to evaluate the transition temperatures using lower bound curves instead of best fit lines even though the use of the two parametric Weibull model /weakest link theory/ would yield overconservative results due to the small data sets evaluation /Wallin, 1984/. There were difficulties encountered when evaluating upper shelf relationship due to the small number of specimens available, only two data points were used to calculate the best fit line in one case, /heat A/, therefore the applicability of obtained values of upper shelf drop is rather limited.

Obtained results in terms of transition temperature shifts for both Charpy impact data and initiation toughness data are well below the maximum acceptable embrittlement limit, Fig. 7., given by:

$$\Delta TT = 29 / F \times 10^{-22} / 1/3$$

With respect to results concerning the value of exponent in this equation, as mentioned earlier, further work is needed to clarify this issue, especially larger data sets analysis.

The correspondence between Charpy impact and initiation toughness test methods in their independent determination of irradiation induced transition temperature shifts is illustrated in Fig. 8. There is a clear tendency of the 41 J temperature shift to overpredict the 100 MPam^{1/2} one, determined from initiation toughness tests. It is recognized, that this is not fully consistent with observations of others, where 1 to 1 correspondence is usually quoted. On the other hand correlations between initiation toughness and Charpy impact energy are purely empirical and opposite tendencies were also reported /Hawthorne, 1985/. Fortunately it could be summarized that transition temperature shifts, determined on 41J level, which is the most commonly used parameter to describe irradiation embrittlement provide a conservative estimate of the "true" transition temperature shift, determined using initiation toughness tests for this type of steel.

7. CONCLUSIONS

Tensile, Charpy impact and fracture properties for 3 heats of both unirradiated and irradiated 15Ch2NMFA GradeAA steel over a range of temperatures are reported.

Considerable effect of specimen size was found in the initiation toughness transition region, despite of it Charpy size specimen could be used as a measure of fracture properties irradiation induced changes.

Recommended equations, describing irradiation embrittlement and hardening are not fully applicable for this type of steel. Further work is needed to clarify this issue with respect to prescribed maximum acceptable embrittlement and saturation effects of irradiation damage occurrence.

Transition temperature shifts, determined from Charpy impact tests were found to be a conservative estimate of shifts measured using initiation toughness tests for this type of steel.

8. ACKNOWLEDGEMENT

This work was carried out in the Nuclear Research Institute, Řež under the sponsorship of the State Comitee for Science, Technology and Investment and the ŠKODA Corporation.

9. REFERENCES

- 1/ Brumovský, M.: Service life of VVER Type Reactor Pressure Vessels. Report ZJE-227, 1987, Škoda Corporation, Plzeň.
- 2/ Bolton, C.J. et.al.: The effect of irradiation on upper shelf fracture toughness of Magnox reactor pressure vessel materials. NEA/UNIPED specialist's meeting on life-limiting and regulatory aspects of core internals and pressure vessels, 1987.
- 3/ Havel, R. et.al.: Teplotní závislost lomové houževnatosti, stanovená na malých zkušebních tělesech. Zpráva ÚJV Řež 8690-M, 1989.
- 4/ Hawthorne, J.R., Menke, B.H., Hiser, A.L.: Notch ductility and fracture toughness degradation of pressure vessel steel reference plates from pool side facility irradiation capsules. ASTM STP 870, F.A. Garner and J.S. Perrin eds., 1985, pp.1163-1186.
- 5/ Ingham, T. et.al.: Influence of specimen size on the upper shelf toughness of SA A533B-1 steel. Proceedings of the 7th SMIRT conference, Vol.G, 1983.
- 6/ Janda, R., Mentl. V.: Lomová houževnatost materiálů TN reaktorů VVER 1000. Proceedings of the 3rd conference: Materiálové a technologické otázky jaderných reaktorů VVER. Srní, 1988.
- 7/ Neale, B.K., Priest, R.H.: The unloading compliance method for crack length measurement using compact tension and pre-cracked Charpy specimens. ASTM STP 856, 1985. pp.375-393.
- 8/ Neale, B.K. et.al.: A procedure for the determination of the fracture resistance of ductile steels, CEGB report TPRD/B/0495/RB4, 1984.
- 9/ NID IAE 443.56-86, INTERATOMENERGO Standard, Odolnost proti křehkému porušení, 1986.
- 10/ Oldfield, W.: Curve fitting impact test data: a statistical procedure. ASTM Standardization News, November, 1975, pp.24-39.
- 11/ Ošmera, B. et.al.: Neutron spectra measurement in VVR-S reactor. Proceedings of the 4th ASTM-EUROATOM symposium on reactor dosimetry. March 1982, NBS, Washington D.C.

12/ Pina, J. et.al.: Ozařování ocelí RIN 1000 v roce 1987. Zpráva ÚJV Řež 8514-M, 1988.

13/ Wallin, K. : The scatter in K_{IC} results. Eng. F. Mech., Vol. 19, No.6, pp. 1085-1093, 1984.

Table 1.: Chemical composition of 15Ch2NMFA Grade AA steel, /wt.%/

Material (heat)	C	Si	Mn	P	S	Ni	Cr	Cu	Mo	V	Sn	As	Sb
A	.17	.29	.41	.009	.009	1.27	2.05	.06	.57	.09	.003	.004	.001
B	.15	.27	.51	.009	.011	1.25	2.10	.03	.56	.07	.001	.003	.001
C	.15	.28	.52	.006	.007	1.27	2.13	.05	.56	.09	.001	.004	.001

Table 2.: Tensile tests results

Material (heat)	F(flucence) $\times 10^{23}$, E>1MeV	R _{p0.2} MPa	$\Delta R_{p0.2}$		R _m MPa	A ₅ %	Z %	B _F
			MPa	%				
A	0	632	-	-	744	19.0	78	-
	1.2	685	53	8	774	18.7	78	23
	4.4	794	162	25	852	17.0	74	46
B	0	528	-	-	641	22.0	82	-
	1.7	640	112	21	715	19.0	77	44
	4.3	726	198	37	779	17.0	76	56
C	0	576	-	-	678	21.0	82	-
	4.6	772	196	34	823	17.5	77	55

Table 3.: Charpy impact tests results

Material (heat)	F(flucence) $\times 10^{23}$, E>1MeV	TT _{41J} C	TT ₀ C	ΔTT_{41J} C	ΔTT_0 C	USE Jcm ²	A _F
A	0	-118	-88	-	-	276	-
	1.2	-79	-69	39	19	249	17
	4.4	-31	-19	87	69	249	25
B	0	-105	-93	-	-	276	-
	2.2	-66	-61	39	32	252	14
	4.3	-23	-15	82	77	238	23
C	0	-105	-87	-	-	276	-
	2.0	-77	-63	28	24	270	10
	3.8	-37	-24	68	63	222	20

Table 4.: Initiation toughness tests results

Material (heat)	F(flucence) $\times 10^{23}$, E>1MeV	TT ₁₀₀ C	ΔTT_{100} C	K _{0.2}	$\Delta K_{0.2}$	A _F ^K
				MPam ^{1/2}		
A	0	-153	-	288	-	22
	4.6	-75	78	239	46	
B	0	-147	-	294	-	14
	4.6	-98	49	275	19	
C	0	-152	-	321	-	12
	4.6	-110	42	284	37	

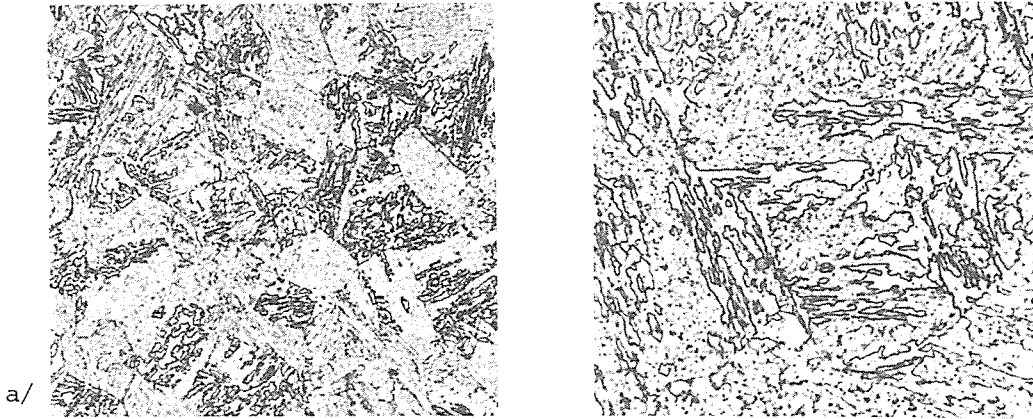


Fig.1: Microstructure of 15Ch2NMFA GradeAA steel, a/ 100 x, b/ 400 x

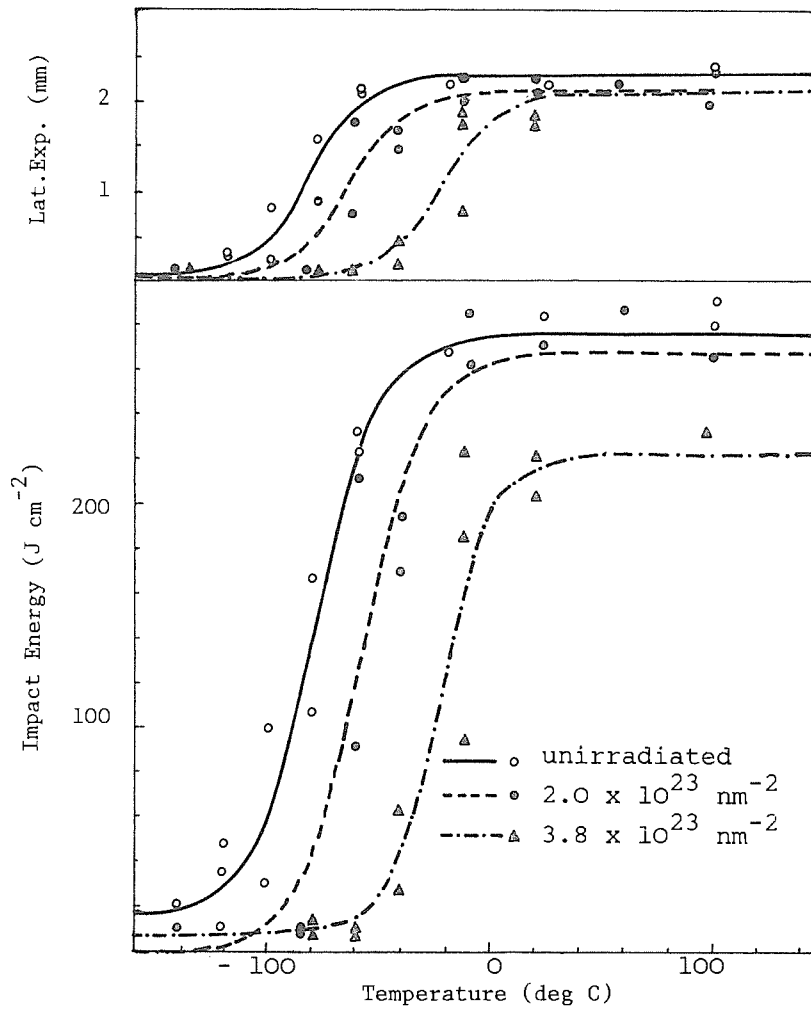


Fig.2: Charpy impact test results, heat C

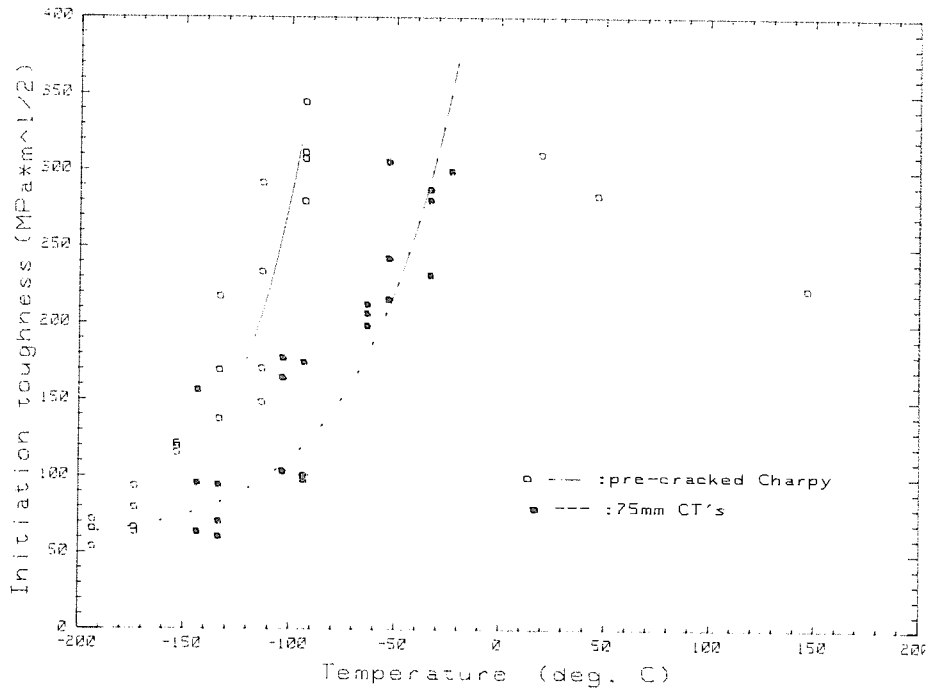


Fig.3: Initiation toughness versus temperature, effect of specimen size.

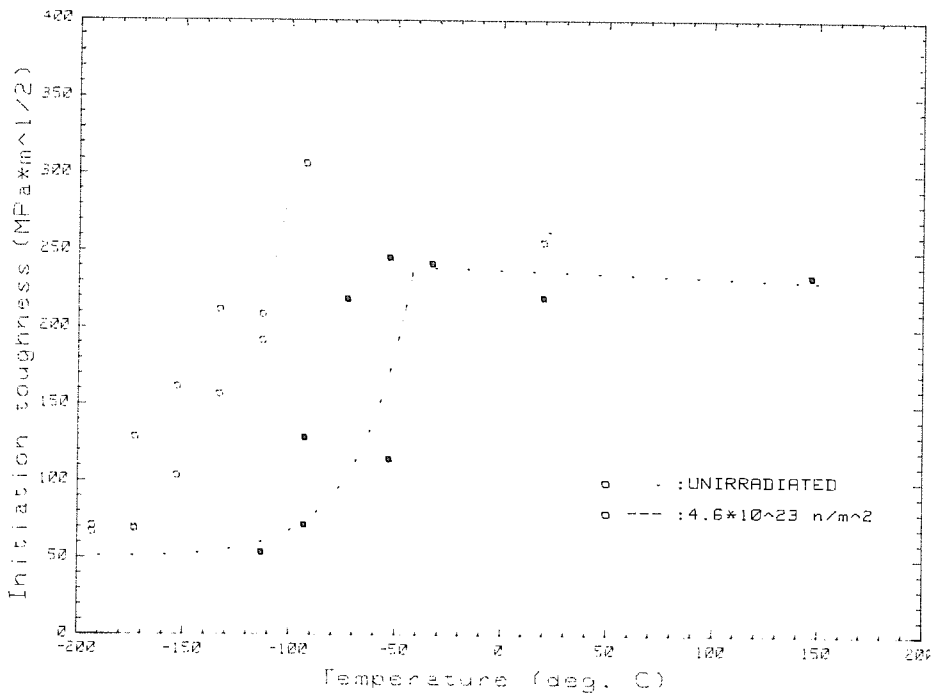


Fig.4: Initiation toughness versus temperature, heat A

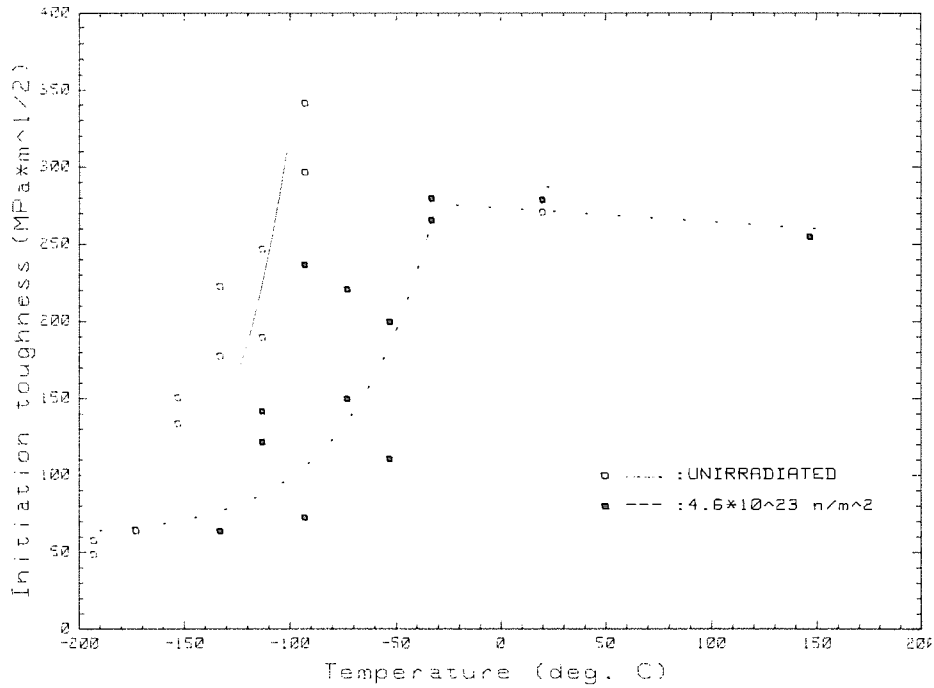


Fig.5: Initiation toughness versus temperature, heat B

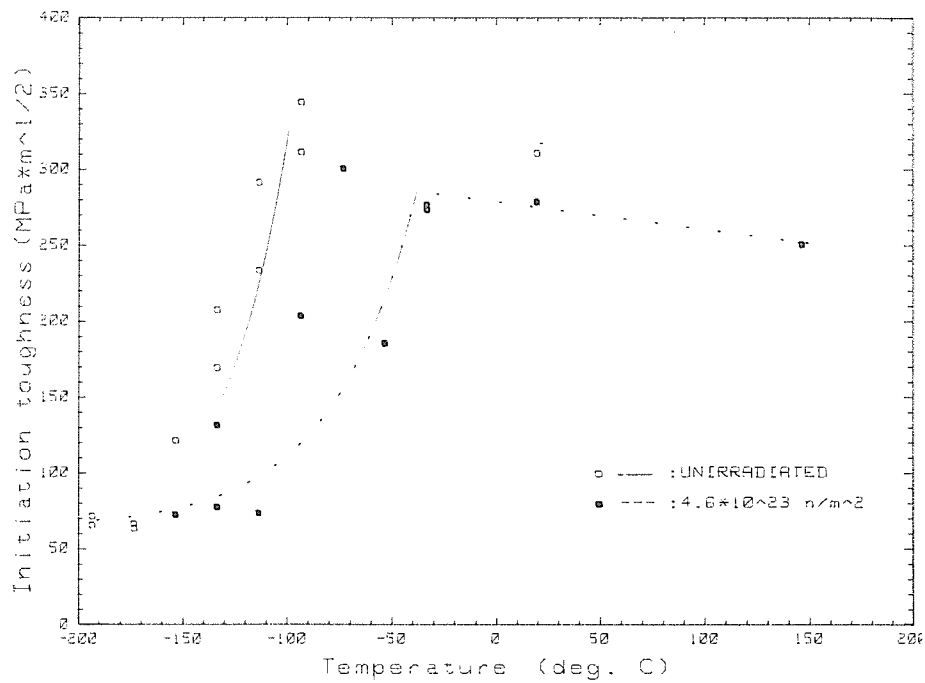


Fig.6: Initiation toughness versus temperature, heat C

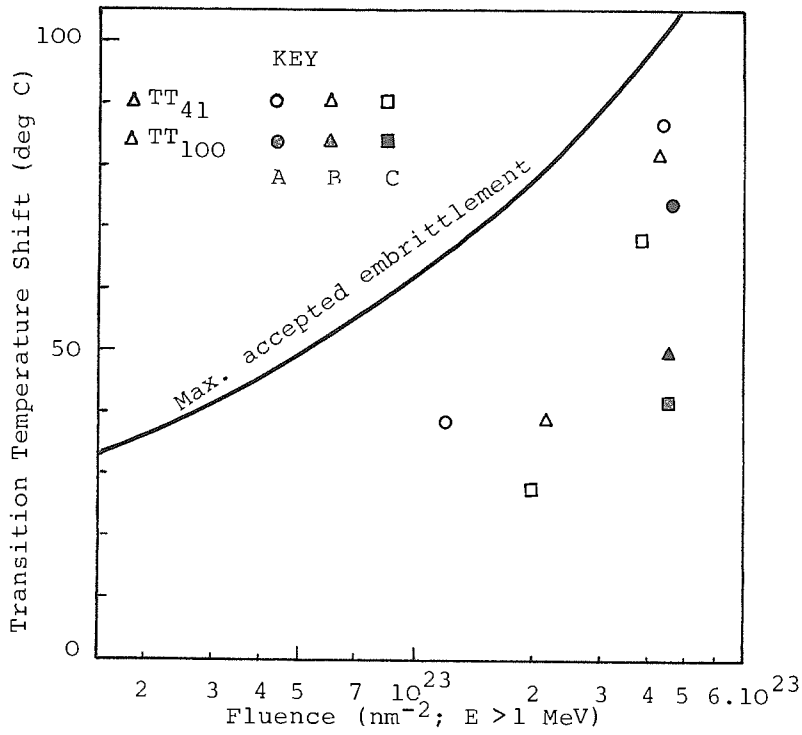


Fig.7: Measured and max. acceptable irradiation embrittlement

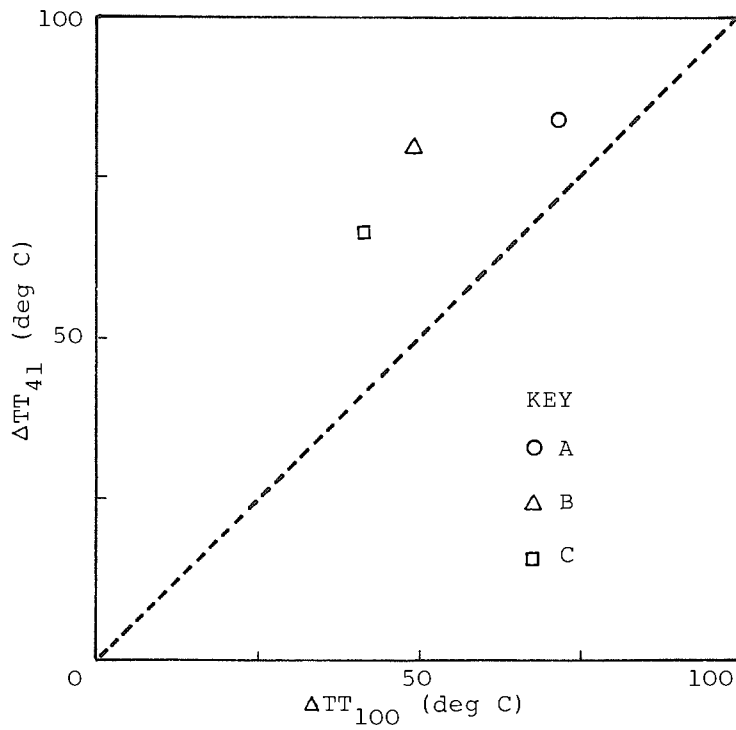


Fig.8: ΔTT_{41} versus ΔTT_{100} correlation

